ACS APPLIED MATERIALS & INTERFACES

Letter

www.acsami.org

Significantly Enhanced Energy Output from 3D Ordered Macroporous Structured Fe_2O_3/Al Nanothermite Film

Wenchao Zhang,[†,‡,*] Baoqing Yin,[†] Ruiqi Shen,[†] Jiahai Ye,[†] Jason A. Thomas,[‡] and Yimin Chao[‡,*]

[†]School of Chemical Engineering, Nanjing University of Science and Technology, Nanjing 210094, China

[‡]School of Chemistry, University of East Anglia, Norwich NR4 7TJ, United Kingdom

Supporting Information

ABSTRACT: A three-dimensionally ordered macroporous Fe_2O_3/Al nanothermite membrane has been prepared with a polystyrene spheres template. The nanothermite, with an enhanced interfacial contact between fuel and oxidizer, outputs 2.83 kJ g^{-1} of energy. This is significantly more than has been reported before. This approach, fully compatible with MEMS technology, provides an efficient way to produce micrometer thick three-dimensionally ordered nanostructured thermite films with overall spatial uniformity. These exciting achievements will greatly facilitate potential for the future development of applications of nanothermites.

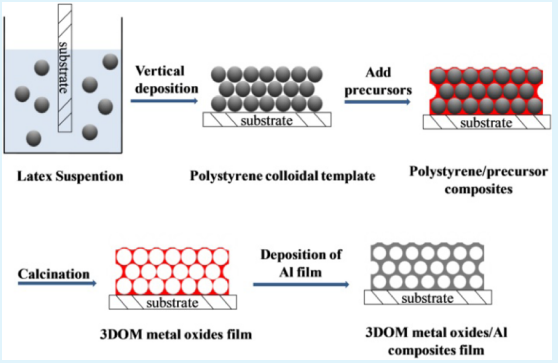

KEYWORDS: *nanoenergetic materials, nanothermite, metastable intermolecular composites, polystyrene spheres template, microelectro-mechanical system*

1. INTRODUCTION

Energetic thermites are a class of substances that store chemical energy and, when ignited, undergo an exothermic reaction without the need for external substances such as oxygen.[1−3] As a consequence of this feature, they are broadly used in propulsion, thermal batteries, welding, material synthesis, waste disposal, and power generation for microsystems.[4] However, one of the limitations of thermites is that their ignition time in conventional mixtures is longer.[5] Nanothermites, also referred to metastable intermolecular composites (MICs), have shown improved performance in terms of faster energy release rate when compared with traditional thermite materials.[2] In MICs, oxidizer and fuel make contact with each other in the nanoscale, thus mass transport limitations between reactants are reduced, which in turn causes an increased burning rate. In the literature, the following three main processes have been employed to synthesize MICs: sol−gel processing,[6,7] multilayered foils,[8−10] and core−shell nanowires.[4,11,12] Sol−gel chemistry produces nanometer sized particles immersed in a solid network. Such structures are macroscopically uniform because of the small particle size and small interparticle separations. However, randomly distributed particles can inhibit self-sustaining reactions by local separation of the oxidizer and fuel.[2,7] Furthermore, organic impurities that make up about 10% of the sample mass during the sol−gel processing result in reduced energy release.[2,7] Multilayered foils consisting of alternating layers of oxidizer and fuel provide large, regular planar interfaces and very close contact between oxidizer and fuel reactants.[13] They are nanoscaled in one dimension and the energy release proceeds through interdiffusion at the interface. However, this fabrication process is time-consuming, expensive, and difficult to scale up.[4] In recent years, one-dimensional nanowires (NWs) have been used in the formation of uniform metal oxide/Al core−shell NWs thermites as templates, followed by the deposition of a layer of Al film around the metal oxide NWs.[4,11−13] Although CuO/Al, NiO/Al and Co_3O_4/Al core−shell structures have been shown to have some advantages when compared with conventional materials, such as enhanced contact, reduced impurities, and easier integration into microsystems.[13] Few different species of NWs structured metal oxides can be made, thus making it difficult to meet the demand for diversity in nanothermites. 3D ordered macroporous (3DOM) materials with uniform pore size and well-defined periodic structure have recently become an important point of scientific focus due to their potential applications in absorbents, catalysts, photonic crystals, and lithium ion anodes.[14−16] To date, almost all the 3DOM metal oxides (oxides of Si, Ti, Zr, Al, Fe, Sb, W, Ni, Cr, Mn, Mg, Zn, Co, Sn, Eu, Sm, Nd, and mixtures of some of these) have been synthesized using a colloidal crystal templating method.[17−19] Therefore, this method provides a foundation for the preparation of different kinds of thermites based on 3DOM metal oxide membranes. However, there is no report in the literature on the deposition of Al onto such 3DOM membranes

Received: November 23, 2012
Accepted: December 31, 2012
Published: December 31, 2012

to form nanothermites. Here we demonstrate a new synthesis approach for energetic thermite membranes consisting of a 3DOM Fe_2O_3 membrane and Al. Al has been shown to be deposited by either a thermal evaporation or a magnetron sputtering method. This approach is fully compatible with MEMS technology. Furthermore, this nanothermite film, which demonstrates enhanced interfacial contact between fuel and oxidizer, can be produced easily and efficiently.

2. EXPERIMENTAL SECTION

The preparation process is as follows: All chemicals purchased from Aladdin-reagent Inc. were reagent grade and used as supplied except for styrene which was freshly vacuum distilled before use. Microslides were used as substrates. The polystyrene spheres were synthesized via an emulsion polymerization method.[20] Typically, 0.04 g of sodium *p*-styrene sulfonate and 0.13 g of $NaHCO_3$ were dissolved in 200 mL of deionized water and stirred for 10 min. Next, 19.6 g of styrene monomers were introduced into the solution under N_2. Then, 0.29 g of potassium persulfate was added to the solution and the whole polymerization system was reacted for 24 h at a constant temperature of 70 °C, to form polystyrene spheres in suspension. Prior to the deposition, the microslide substrate was rinsed with hydrochloric acid, acetone and then anhydrous ethanol, followed by drying in a convection oven. A vertical deposition method was then employed to assemble polystyrene spheres onto the microslide substrate, whereby a clean microslide was immersed vertically into about 30 mL of a suspension of polystyrene spheres in latexand dispersed ultrasonically. This apparatus was dried in a temperature-controlled furnace at 45 °C for 36 h. A three-dimensionally ordered latex template was then obtained, as shown in Scheme 1.

Scheme 1. Schematic of the Synthesis Procedure for 3DOM Nanothermite Film

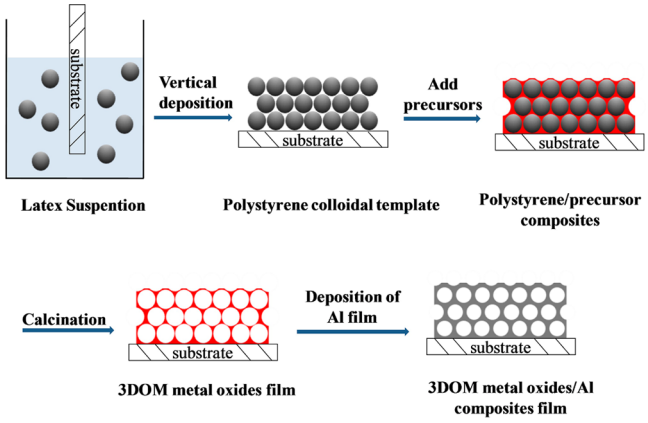

The precursor solution was prepared using $Fe(NO_3)_3{\cdot}9H_2O$ (1.5 mol L^{-1}), which was dissolved in ethylene glycol. After the polystyrene spheres template was immersed in the precursor solution for 10 min the sample was drawn upward vertically at a speed of 1 cm min^{-1}. It was then immediately placed in a drying oven for 1 h at 50 °C. This process was then repeated once more in order to ensure that the polystyrene spheres template was fully infiltrated. The sample was stored at room temperature overnight and then placed in a tube furnace. The temperature was raised at a rate of 1 °C min^{-1} to 500 °C and was then held steady for 5 h. Through this process a thin film of 3DOM α- Fe_2O_3 with thickness of about 1.4 μm was formed on the substrate. Al was deposited onto the substrate with α-Fe_2O_3 membrane by thermal evaporation or magnetron sputtering at a vacuum of 5×10^{-2} Pa. During the deposition, the substrate temperature and deposition rate were maintained at 30 °C and 0.5−1.0 Å s^{-1} respectively. The deposition duration was 1 h. The weight of product produced in this process depends upon the surface area of the substrate and the height of the polystyrene template. The deposition of Al is a standard MEMS technique; therefore, it is a scalable process.

The morphology of all the samples was examined by a field-emission SEM (Hitachi, S-4800). The crystal structures were analyzed by using XRD (Bruker, D8Advance). DSC measurement was performed with a heating rate of 20 °C·min^{-1} under a 30.0 mL min^{-1} N_2 flow on a sample of mass 4.0789 mg (METTLER TOLEDO, DSC 1).

3. RESULTS AND DISCUSSION

The morphologies of the polystyrene spheres template deposited onto the microscope slide substrate, the 3DOM Fe_2O_3 membrane and Fe_2O_3 membrane after Al deposition were examined by field-emission scanning electron microscopy (SEM), as shown in Figure 1. Images a and b in Figure 1 show

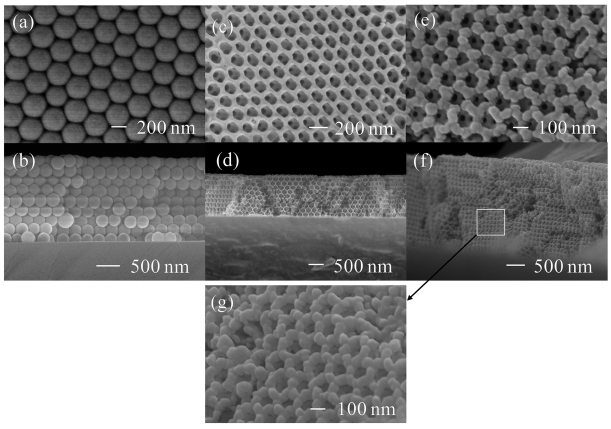

Figure 1. SEM images of (a, b) polystyrene spheres template, (c, d) 3DOM α-Fe_2O_3 membrane, and (e, f) Fe_2O_3/Al membrane after Al deposition; (a, c, e) surface view and (b, d, f) cross-section view, (g) zoom view from the white square in f.

the surface and cross-section of the polystyrene spheres template. In Figure 1a, each 280 nm sphere can be seen to be surrounded by six others in one plane, indicating a hexagonal array in a face-centered cubic close-packed structure. Nine layers of the polystyrene spheres template with thickness of about 1.8 μm in total can be seen in the cross section in Figure 1b. The thickness of the polystyrene spheres template is easily controlled by the concentration of suspension.

Figure 1c shows a surface view of the 3DOM Fe_2O_3 membrane produced by immersing the polystyrene spheres template into the precursor solution and calcining in a tube furnace. The morphology of 3DOM Fe_2O_3 indicates a hexagonal honeycomb structure surrounded by six other hexagons with a wall thickness of 31.4 nm. The hexagon is not regular, and deformation of the polystyrene spheres template during the calcination is likely to be the main cause of this irregularity.[21] Figure 1d lays out a cross-section view of the Fe_2O_3 membrane. It can be observed that the Fe_2O_3 membrane has nine layers, which is consistent with the

dx.doi.org/10.1021/am302815y | ACS Appl. Mater. Interfaces 2013, 5, 239−242

polystyrene spheres template. The thickness is only 1.4 μm, as opposed to the 1.8 μm template. This difference is caused by the deformation of the polystyrene spheres template during the calcination. The measured specific surface area of this oxide film is 44.5898 $m^2\ g^{-1}$.

Images e and f in Figure 1 are top and cross-section view SEM images of the 3DOM α-Fe_2O_3 membrane after the Al deposition. The cross-section was made from the sample after the Al deposition. Figure 1g)is a detailed enlargement of the main image f. It is clear that nano Al is coated on the 3DOM α-Fe_2O_3 structure to form a core−shell nanostructure, which enhances the interfacial contact and improves the reactivity. The wall thickness becomes approximately 65−92 nm, as compared with the 31.4 nm thickness before Al deposition. The cross section view SEM images show that nano Al is not only deposited onto the surface of Fe_2O_3 membrane, but is also integrated around the middle and bottom of the membrane. Thus, it can be confirmed that Al vapor can easily enter into the 3DOM structure and the method of Al deposition is feasible. EDX analysis shows an atomic ratio of Al to Fe of 1.18 to 1, where the overdose of Al is to compensate the oxidation of Al, see Figure S1 and Table S1 in the Supporting Information. It is worth noting that the pores of Fe_2O_3 could not be fully filled by Al. The result of this is that the membrane has a lower energy density than that of a fully dense system.

The membranes were analyzed by X-ray diffraction (XRD) after the calcination process, after Al deposition and finally after the differential scanning calorimetry (DSC) test. The typical XRD patterns are shown in Figure 2. Four intense peaks are

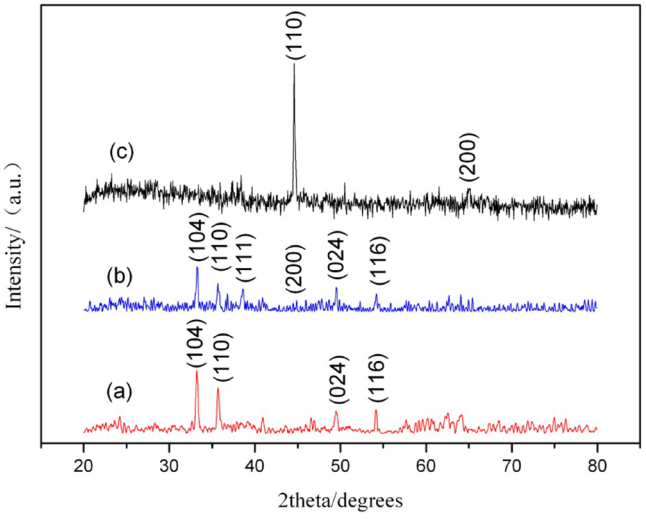

Figure 2. XRD patterns of (a) 3DOM α-Fe_2O_3 membrane after calcination, (b) Fe_2O_3/Al membrane, (c) Fe_2O_3/Al membrane after a DSC test.

observed at 33.2, 35.7, 49.5, and 54.1° in Figure 2a, corresponding to planes (104), (110), (024), and (116), which indicate that Fe_2O_3 is formed after calcination.[22] From Figure 2b, it can be seen, as expected, that there are two Al peaks at 38.6 and 44.9° as a consequence of the Al deposition.[23] The XRD pattern of the Fe_2O_3/Al membrane reveals no unknown crystalline phases or visible impurities. Figure 2c shows the XRD spectrum of the Fe_2O_3/Al membrane after a DSC test. Compared with Figure 2b, it can be seen that the peaks of Fe_2O_3 and Al have vanished and a dominant peak at 44.6° corresponds to Fe plane (110).[24] This means Fe_2O_3 has been reduced by Al. The patterns of Al_2O_3 are not visible from Figure 2c, because Al_2O_3 polymorphs produced in the reaction are amorphous or poorly crystalline.[4,25]

As most energetic applications require some form of self-propagation, a photo has been obtained during the burning, see Figure S2 in the Supporting Information. To evaluate the heat release of the reaction, we characterized the Fe_2O_3/Al membrane with DSC in the temperature range 100 to 900 °C, as shown in Figure 3. It can be observed that there are two

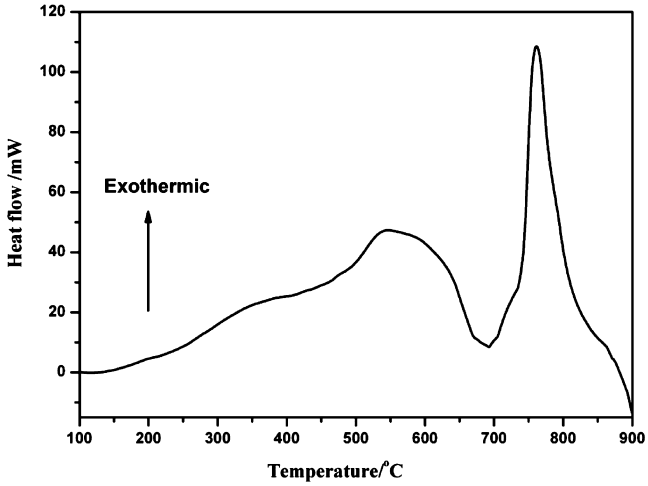

Figure 3. DSC curve of Fe_2O_3/Al membrane obtained in a temperature range from 100 to 900 °C with a heating rate of 20 °C min^{-1} under a 30.0 mL min^{-1} N_2 flow.

exotherms in the DSC curve. The trend of the curve is similar to that of self-assembled Fe_2O_3 nanotubes−Al nanoparticles reported by Cheng et al.[26] The first exotherm rises slowly with a peak temperature at 548 °C. This means that the nanoscale Fe_2O_3/Al membrane can react mildly below the melting point of Al, 660 °C. In comparison with the peak temperature at 588 °C observed by Cheng et al, a lower peak temperature of 548 °C is shown in Figure 3. This is due to the more compact interfacial contact between Fe_2O_3 and Al. The second exotherm rises more abruptly with a peak temperature of 770 °C. This suggests that the Fe_2O_3/Al membrane has a faster release speed of heat when Al has melted. Insufficient Al may result in the second exothermic peak being lower, as shown in Figure S3 in the Supporting Information, which is in consistent with the results from self-assembled samples.[26] Through integration of the two exothermic peaks of the DSC measurement, from 480 to 638 °C and 735 to 813 °C, it can be observed that the outputs of heat are 902 J g^{-1} and 1929 J g^{-1}, respectively. The total heat release is 2.83 kJ g^{-1}.High heat evolution of the reaction is shown to be caused by two factors. First, by virtue of few impurities being introduced during the synthesis: fewer impurities exist due to certain processes, for example: organic substances can be effectively removed by calcination; there is also a decreased probability that Al will be oxidized when it is evaporated in vacuo. The second factor to consider is the compact interfacial contact between fuel and oxidizer, evidenced by the large specific surface area, which results in high energy release. The Fe_2O_3 prepared has a three-dimensionally ordered macroporous structure and can provide an excellent template for the uniform coating and distribution of Al. Although the nanothermite is broken into pieces during the DSC tests, each section is still a uniform Fe_2O_3/Al mixture

dx.doi.org/10.1021/am302815y | ACS Appl. Mater. Interfaces 2013, 5, 239−242

so it can entirely react. Hence, the current Fe_2O_3/Al membrane significantly improves the overall spatial uniformity and heat evolution of the nanothermites.

4. CONCLUSIONS

In summary, the microstructure with open and interconnected macropores of 3DOM Fe_2O_3/Al nanothermite films were successfully synthesized with a polystyrene spheres template. These films have three-dimensionally ordered macroporous structure with overall spatial uniformity and compact interfacial contact between fuel and oxidizer, which significantly enhances energy output. The method, fully compatible with MEMS technology, provides an efficient way to produce micrometer-thick nanostructured thermite films. We anticipate this exciting achievement will greatly facilitate the future of nanothermites and their potential applications.

■ ASSOCIATED CONTENT

Supporting Information

Video and photograph of thermal ignition of 3DOM Fe_2O_3/Al nanocomposite, EDX analysis, and DSC curve of Fe_2O_3/Al membrane with less Al deposition duration. This material is available free of charge via the Internet at http://pubs.acs.org

■ AUTHOR INFORMATION

Corresponding Author

*E-mail: zhangwenchao303@yahoo.com.cn (W.Z.); y.chao@uea.ac.uk (Y.C.).

Notes

The authors declare no competing financial interest.

■ ACKNOWLEDGMENTS

This work was supported by the National Science Foundation of China (NSFC, Grant 50806033), Chinese Postdoctoral Science Foundation (Grant 2012M511285) and EPSRC under Grant EP/G01664X/1.

■ REFERENCES

(1) Kim, S. H.; Zachariah, M. R. *Adv. Mater.* **2004**, *16*, 1821.
(2) Rossi, C.; Zhang, K.; Esteve, D.; Alphonse, P.; Tailhades, P.; Vahlas, C. *J. Microelectromech. Syst.* **2007**, *16*, 919−931.
(3) Séverac, F.; Alphonse, P.; Estève, A.; Bancaud, A.; Rossi, C. *Adv. Funct. Mater.* **2012**, *22*, 323−329.
(4) Ohkura, Y.; Liu, S.-Y.; Rao, P. M.; Zheng, X. *Proc. Combust. Inst.* **2011**, *33*, 1909−1915.
(5) Stamatis, D.; Jiang, Z.; Hoffmann, V. K.; Schoenitz, M.; Dreizin, E. L. *Combust. Sci. Technol.* **2008**, *181*, 97−116.
(6) Prakash, A.; McCormick, A. V.; Zachariah, M. R. *Chem. Mater.* **2004**, *16*, 1466−1471.
(7) Tillotson, T. M.; Gash, A. E.; Simpson, R. L.; Hrubesh, L. W.; Satcher, J. H.; Poco, J. F. *J. Non-Cryst. Solids* **2001**, *285*, 338−345.
(8) Anselmi-Tamburini, U.; Munir, Z. A. *J. Appl. Phys.* **1989**, *66*, 5039.
(9) Blobaum, K. J.; Reiss, M. E.; Plitzko, J. M.; Weihs, T. P. *J. Appl. Phys.* **2003**, *94*, 2915.
(10) Petrantoni, M.; Rossi, C.; Salvagnac, L.; Conédéra, V.; Estève, A.; Tenailleau, C.; Alphonse, P.; Chabal, Y. J. *J. Appl. Phys.* **2010**, *108*, 084323.
(11) Zhang, K.; Rossi, C.; Ardila Rodriguez, G. A.; Tenailleau, C.; Alphonse, P. *Appl. Phys. Lett.* **2007**, *91*, 113117.
(12) Zhang, K.; Rossi, C.; Alphonse, P.; Tenailleau, C.; Cayez, S.; Chane-Ching, J. Y. *Appl. Phys. A: Mater. Sci. Process.* **2009**, *94*, 957−962.
(13) Xu, D.; Yang, Y.; Cheng, H.; Li, Y. Y.; Zhang, K. *Combust. Flame* **2012**, *159*, 2202−2209.
(14) Deutsch, M.; Vlasov, Y. A.; Norris, D. J. *Adv. Mater.* **2000**, *12*, 1176−1180.
(15) Holland, B. T. *Science* **1998**, *281*, 538−540.
(16) Chu, Y.; Pan, Q. *ACS Appl. Mater. Interfaces* **2012**, *4*, 2420−5.
(17) Sadakane, M.; Asanuma, T.; Kubo, J.; Ueda, W. *Chem. Mater.* **2005**, *17*, 3546−3551.
(18) Sadakane, M.; Horiuchi, T.; Kato, N.; Takahashi, C.; Ueda, W. *Chem. Mater.* **2007**, *19*, 5779−5785.
(19) Holland, B. T.; Blanford, C. F.; Do, T.; Stein, A. *Chem. Mater.* **1999**, *11*, 795−805.
(20) Kim, J. H.; Chainey, M.; El-Aasser, M. S.; Vanderhoff, J. W. *J. Polym. Sci., Part A: Polym. Chem.* **1992**, *30*, 171−183.
(21) Xia, Y. N.; Gates, B.; Yin, Y. D.; Lu, Y. *Adv. Mater.* **2000**, *12*, 693−713.
(22) Yadav, B. C.; Singh, S.; Yadav, A. *Appl. Surf. Sci.* **2011**, *257*, 1960−1966.
(23) Chu, M. S.; Wu, S. K. *Acta Mater.* **2003**, *51*, 3109−3120.
(24) Cheng, R.; Zhou, W.; Wang, J. L.; Qi, D.; Guo, L.; Zhang, W. X.; Qian, Y. *J. Hazard. Mater.* **2010**, *180*, 79−85.
(25) Umbrajkar, S. M.; Schoenitz, M.; Dreizin, E. L. *Thermochim. Acta* **2006**, *451*, 34−43.
(26) Cheng, J. L.; Hng, H. H.; Lee, Y. W.; Du, S. W.; Thadhani, N. N. *Combust. Flame* **2010**, *157*, 2241−2249.